Interdecadal
Changes in SST Variability Drivers
in the Senegalese-upwelling: The Impact of ENSO

Malick Wade[(1)], Belén Rodríguez-Fonseca[(2,3)], Marta Martín-Rey[(2,3,6)], Alban Lazar[(4)], Jorge López-Parages[(5, 6),] and Amadou Thierno Gaye[(7)]

(1) Laboratory of Physics of the Atmosphere and Ocean Science (LSAO), Gaston Berger University, Senegal

(2) Instituto de Geociencias IGEO UCM-CSIC, Madrid

(3) University Complutense de Madrid, Spain

(4) Sorbonne University, UPMC, LOCEAN Laboratory, 4 place Jussieu, F-75005 Paris, France

(5) CERFACS, Modelling and Global Change Team, Toulouse, France

(6) Instituto de Ciencias del Mar (ICM), CSIC, Barcelona, Spain

(7) Laboratory of Physics of the Atmosphere and Ocean Simeon Fongang (LPAO-SF), Dakar, Senegal

Corresponding Author:
Malick Wade
Laboratoire des Sciences de l'Atmosphère et de l'Océan
Université Gaston Berger de Saint-Louis, BP 1325, route Gallèle, Senegal
Tel: +221 77 825 93 64
Fax: +221 77 825 93 64
Email: malick.wade@ugb.edu.sn
ORCID: 0000-0002-8270-4110

Abstract

Sea Surface Temperature (SST) variability in the North Eastern Tropical Atlantic has its center of action in the Senegalese-Mauritanian upwelling system, where its drivers are wind-induced ocean dynamics and air-sea thermodynamic processes. Thus, a better understanding of the local wind variations, together with their predictability, contributes to a more comprehensive assessment of the SST variability in that region. In this study, we use monthly data from two ocean reanalyses, SODA and ORAS-5, and a regional forced-ocean simulation to characterize the interannual SST variability off the Senegalese Coast in the common period 1960-2008. Local indices of the mixed layer heat budget during the major upwelling season (February-March-April) exhibit pronounced interannual to decadal variability. We demonstrate that the local interannual SST variability undergoes inter-decadal fluctuation and concomitant changes in its local and remote drivers. Off-Senegal SST variability was largely controlled by wind-induced Ekman transport during the 1960s-1970s, acting under favorable thermocline and mixed layer conditions. However, from 1980s onwards, the drastically reduced Ekman impact observed on local SSTs is associated with a deeper thermocline. This shift in the effectiveness of the dynamic mechanisms coincides with a more active ENSO teleconnection with upwelling before the 1980s. An extended SODA record reveals that the multidecadal modulator of the ENSO impact on the North-eastern Tropical Atlantic resembles the negative phase of the Atlantic Multidecadal Variability. Our results bring to light the fundamental role played by the global

decadal background state in the activation of the drivers and air-sea mechanisms responsible for generating the interannual off-Senegal SST variability.

Keywords: ENSO, Eastern North Tropical Atlantic, Senegalese upwelling, interannual teleconnection.

1. Introduction

The ocean circulation in the North Eastern Tropical Atlantic is dominated by a broad and weak southward boundary current, known as the Canary Current, which forms the eastern limb of the North Atlantic subtropical gyre, and by a strong upwelling system triggered by the trade winds. Coastal and off-shore upwelling results from these northeasterly winds, which drive a zonal Ekman transport under the action of the Coriolis force (Jacox et al., 2018). This transport is indeed divergent and particularly strong at the coast, but also in the ocean interior over a distance depending on latitude (Faye et al., 2015). Mass balance requires compensation by an upward vertical transport of cold and nutrient-rich waters, which favors phytoplankton growth (Herbland and Voituriez1974; Huntsman and Barber 1977; Bricaud et al., 1987; Van Camp et al., 1991). The variability of phytoplankton biomass is therefore associated with the variability of the thermocline nutrient stock and the intensity of the overall upwelling system. Consequently, the scientific community has made considerable efforts to gain a better understanding of the processes behind the upwelling variability as well as its local and remote drivers. A good indicator of coastal upwelling is the Sea Surface Temperature (SST) along the coast. At short timescales, anomalous cold events generally occur a few days after upwelling-favorable wind stress events (Van Camp et al., 1991; Ndoye et al., 2014). The linkage between wind stress and coastal upwelling, from seasonal to interannual timescales, has also been confirmed using historical reports (Wooster et al., 1976), satellite data and ocean reanalysis (Van Camp et al., 1991; Nykjaer and Van Camp 1994; Santos et al., 2005; Castelao and Wang 2014; Cropper et al., 2014).

The relatively cold and nutrient-rich upwelled coastal waters mostly flow at specific locations along the North-West African coast, the most prominent off Cape Blanc and off Cape Verde peninsula, south of Dakar, which is the most westward location of the African continent. In particular, the coast of Senegal, which extends between 12°N and 17°N, houses the southern flank of the Canary Current Upwelling System (CCUS); that is, the so-called Senegalese Coastal Upwelling (hereinafter SCU). The SCU system is characterized by a marked seasonality, the boreal late winter and early spring (February-March-April, FMA) being the season with the strongest upwelling intensity, which occurs due to the intense trade winds and the southward migration of the ITCZ (Cropper et al., 2014; Faye et al., 2015).

Although anomalous upwelling largely controls the SST variability over the North-West African upwelling region, Wind-Evaporation-SST (WES) feedback (Xie and Philander, 1994) may also contribute, since it is one of the major drivers of SST variability in the Tropical North Atlantic Ocean (Polo et al., 2005; Chang et al., 1997; Amaya et al., 2017). The boundary layer WES feedback is a purely thermodynamic mechanism which, in the deep tropics, works as follows: consider an anomalous interhemispheric northward positive (negative) SST gradient. This generates anomalous northward (southward) cross-equatorial surface winds because of the development of an anomalous positive (negative) sea level pressure gradient. The induced cross-equatorial winds turn eastward (westward) on the northern (southern) side of the equator due to the Coriolis force, thereby reducing (enhancing) the background northeasterly (southeasterly) winds. Consequently, evaporation tends to decrease (increase), which further enhances (reduces) the SST and amplifies (reducing) the initial SST gradient.

It is important to remark that these air-sea thermodynamic processes have been suggested as playing a leading role in controlling the coastal SST variability, triggering local SST modes such as the Dakar Niño (Oettli et al., 2016), although entrainment is not negligible in the case of cold events (Dakar Niñas). This feature contrasts with the dynamic nature of SST variability along upwelling systems, which has been linked to thermocline depth variations associated with ocean wave propagation in the South (Florenchie et al., 2003; Lübbecke et al., 2010; Illig and Bachellery, 2019) and in the North Tropical Atlantic (Diakhate et al., 2016).

Despite their differences, both dynamic (upwelling) and air-sea thermodynamic processes are driven by surface winds, which can be triggered by local or remote forcings (Enfield and Mayer 1997; Polo et al., 2005). In particular, El Niño-Southern Oscillation (ENSO) exhibits a pronounced impact on anomalous SSTs over the Tropical North Atlantic (TNA, Taschetto et al., 2016; Amaya and Foltz, 2014; Lee et al., 2008; Alexander and Scott, 2002; Enfield and Mayer, 1997). The ENSO-TNA teleconnection has been widely investigated and involves changes in the atmospheric Rossby wave-trains in the upper troposphere (Enfield and Mayer, 1997), alterations in the overturning zonal and meridional atmospheric cells (Walker and Hadley cells; see e.g. Wang et al., 2002a), and the excitation of an anomalous Gill-type response over the Amazon basin (García-Serrano et al., 2017), all of which impact on the TNA. A pioneer work by Roy and Reason (2001) showed a significant correlation between ENSO and West African coastal SSTs as well as a strong effect on the primary production in the area. Additional studies have also found a link between ENSO and coastal SST variability via thermodynamic processes (Oettli et al., 2016), and a potential contribution of coastal-poleward propagation of equatorial Kelvin waves in the upwelling circulation through changes in the thermocline depth and wind patterns (Kessler et al., 1995; McPhaden1999; Zhang 2001; Polo et al., 2008; Diakhate et al., 2016).

Previous studies did not separate the processes involved in the SST variability of the North-West African upwelling system in terms of local and remote basin precursors. Moreover, the role played by the ocean mean state conditions in the local SST variability is still poorly understood. A recent study suggests that the ocean background state may modify the effectiveness of the different thermodynamic and dynamic feedbacks involved, and hence the stationarity of the ENSO teleconnection with the SSTs off North-West Africa (Martín-Rey et al., 2018).

A more comprehensive study, including the identification of local and remote drivers of SST variability in the SCU region, remote impacts from ENSO and the stability of these relations, has yet to be conducted.

In this context, the present study investigates the processes behind the interannual SST variability within the SCU during the coldest upwelling season (FMA). The goal of this research is to determine the dynamic vs thermodynamic precursors of coastal SST variability off-Senegal and to quantify the role of Ekman induced upwelling in SST variability. This wind-induced upwelling is compared with the contribution of air-sea fluxes and the ocean precondition (i.e. thermocline and mixed layer depth) throughout the observational record.

The non-stationary behavior of the thermodynamic and dynamic feedbacks is also explored using a set of ocean reanalyses and an ocean-forced regional simulation. In particular, the main questions we address are:

1°) What is the role played by local and remotely-forced surface winds in the SST variations within the SCU region during the last century?
2º) What are the relative contributions of the air-sea thermodynamic vs dynamic processes to the SST variability in the region under study?
3°) Are these contributions stationary in time? Does the ocean background state modulate the mechanisms responsible for generating the local SST variability?
4º) What is the role of ENSO in creating the SCU SST variability? Is the ENSO impact stable throughout the observational record? Is there a link between changes in the ocean background state and ENSO effectiveness in altering the upwelling?

We are especially interested in detecting periods in which SST variability is led by coastal upwelling due to the higher impact on marine ecosystems and fisheries, but also in its link with ENSO due to its impact on the seasonal predictability of this important phenomenon.
The paper is structured as follows: In Section 2, the datasets and methodology used in the present study are described. Results are shown and examined in Section 3, in which we analyze in detail the seasonal cycle (subsection 3.1) and interannual variability (subsection 3.2) of the different variables involved in SCU SST variability. The major contributors to the interannual SST variability and their periods of strong influence are also identified and discussed (subsection 3.3). We then determine the ENSO-related contributors to the local SST variability (subsection 3.4) and explore its non-stationary behavior throughout the 20th century (subsection 3.5). Finally, the main conclusions are summarized in Section 4.

2. Data and Method

2.1 Observations and reanalysis

In order to study the SCU variability and its stationarity, we use version 2.2.4 of the monthly Simple Ocean Data Assimilation (SODA) reanalysis from 1871 to 2008 (Giese and Ray 2011). SODA is an oceanic reanalysis based on the Parallel Ocean Program (POP) physics and forced by surface winds of the 20th Century Reanalysis (20CRv2, hereafter). This extensive ocean reanalysis considers the assimilation of observed 3-D temperature and salinity from hydrographic profile data and ocean stations. The SODA dataset consists of gridded state variables for the global ocean, as well as several derived fields, mapped onto a uniform 0.5°x0.5° longitude-latitude grid with 40-z levels expanding from 5m up to 5000m.

Due to some well-known caveats found in the long SODA dataset (Carton et al., 2018), we also use the ECMWF ocean reanalysis ORAS-5 (Zuo et al., 2019) that covers the period 1958-2018. Notice that the ensemble mean of the 5 members from 1979 onwards is considered, while a single realization is available for the backward extension (1958-1978). Compared to the previous version ORAS4, the new ORAS-5 reanalysis has been performed with the updated version 3.4 of the ocean NEMO model, including an eddy-permitting resolution (0.25^{o}) in the horizontal and 75 vertical levels with a much finer 1-m resolution near the surface (24 levels in the upper 100m). The NEMO model has been forced with surface air-sea fluxes from ERA40 (Uppala et al., 2005) prior to 1979, ERA-Interim (Dee et al., 2011) for the period 1979-2014, and ECMWF operational numerical weather prediction from 2015 onwards. In addition, SODA v3.4.2 is also used to test the results for the last period, as this data base is only available from 1980 to 2018 and does not allow us to infer causes for multidecadal modulations.

Wind stress data, Sea Surface Temperature (SST), mixed layer depth (MLD), thermocline depth (THD), and net surface heat fluxes (NHF) are considered from SODA (1900-2008 period) and ORAS-5 (1958-2018 period) to study the variability of the upwelling within the SCU. Notice that MLD and THD have been derived from the 3-D temperature and salinity fields. The former is computed as the depth at which the density change from the surface is 0.125 (Monterey and Levitus1997) and the latter is defined as the depth of the 18°C isotherm. This isotherm is chosen because it is the most representative thermocline proxy over the African coastlines, particularly within upwelling areas where the isotherms outcrop (Polo et al., 2008).

Regarding the air-sea fluxes, net heat flux is provided as an output for the ORAS-5 reanalysis, while for the SODA reanalysis it is taken from the 20CRv2 dataset (Compo et al., 2011), the atmospheric reanalysis used to force this long assimilation run.

2.2 ATLTROP025 model interannual simulation

For a better understanding of the wind-driven physical processes at work and possible modulations, an interannual simulation with the ocean NEMO model (Martín-Rey et al. 2019) has been also used and analyzed in the present study. Using these simulations, we can analyze how the ocean responds to the atmospheric forcing, which in our case, we will see that is seems to come, during some particular periods, remotely from ENSO.
The atmospheric forcings (air-sea fluxes) are taken from the DFS4.4 datasets (Broudeau et al. 2010), and the model configuration is restricted to the Tropical Atlantic region [58W-18W, 31N-30S]. The horizontal resolution is ¼ and has 46-z vertical levels. The period of the interannual simulation (NEMO-INT hereafter) extends from 1960 to 2011. This interannual simulation started from initial stable conditions taken from a stabilized climatological run.

The NEMO-INT realistically captures the mean and the interannual variability of the North-West African upwelling, with small biases in the annual mean of SST and thermocline depth (see Fig. 1 in Martín-Rey et al., 2019). Thus, this simulation provides a realistic scenario for investigating the role of surface winds in triggering dynamic (Bjerknes feedback and upwelling) and thermodynamic mechanisms in the study area.

2.3 Methodology

For each of the available years, we begin by computing all possible 3-month seasonal averages (from January-February-March-JFM up to October-November-December - OND) of SST anomalies in the SCU region. The corresponding anomalies are obtained by subtracting the long-term mean of the seasonal averages.
The SCU extension and variability are obtained in terms of the SST annual standard deviation, the maximum variability to the south of the main geographical capes being found throughout our study region (Fig. 1). In particular, this region is used here to calculate a set of indices characterizing the SCU (see white boxes in Fig. 1). The region is embedded in the northern and southern Senegalese coastal upwellings, which are slightly different in terms of intensity mainly due to the configuration of the wind pattern in relation to the geometry of the western Senegalese coast. However, we do not distinguish between the northern and southern Senegalese coastal upwellings since they present broadly the same dynamics.

The Ekman transport along the coast leads to the upwelling of deep cold waters. The Ekman transport (M_e) in terms of wind stress is defined as:

$$\overrightarrow{M_e} = \frac{\tau_y}{\rho f}\vec{i} - \frac{\tau_x}{\rho f}\vec{j} \qquad [1]$$

where $\vec{\tau} = (\tau_x, \tau_y)$ is the wind stress vector, ρ is the density, and f the Coriolis parameter.

Within the SCU, the zonal component of the wind stress is very small and can be reasonably neglected (Fig. 1). Thus, the resultant transport is largely dominated by its zonal component. Furthermore, we also neglect the open ocean divergence of Me, which is significantly smaller than the one at the coast. Hence, in the present study, we define the upwelling index (UI) as the zonal Ekman transport (reversed in sign) averaged along the coast [17°W-18°W, 12°N-16°N], as indicated in Fig. 1 (Bakun, 1973; Sylla et al., 2019):

$$UI = \frac{-\tau_y}{\rho f} \qquad [2]$$

Preliminary analyses on individual maps of 3-month averaged SSTs reveal that February-March-April (hereafter, FMA) exhibits the strongest variability, which is located between 12°N and 16°N (Fig 2.b).

Please note that positive (negative) values of UI correspond to southward (northward) surface winds and upwelling (downwelling) conditions. This zonal Ekman transport also exhibits maximum variability in FMA (Fig. 2a) for ORAS5 and NEMO. In SODA, the values do not differ, although the strong variability occurs in JAS.

Atmospheric and oceanic variables are analyzed in order to understand SST variability in the SCU (Table 1). Furthermore, different filters are applied throughout this study in order to focus on the time scale of interest in each particular case. We filter out the sub-seasonal variability by calculating 3-months running means, and focus then on the maximum upwelling season, that is, FMA. The resultant seasonal average is linearly detrended and filtered with a lanczos filter (Duchon1979; Wilks, 2011) in order to separate interannual and decadal frequencies. Since we wish to focus on the interannual variability of the region, we apply a high-pass filter with a cutoff frequency of 8 years. Note that in the case of the Tropical Pacific SSTs, for example, this procedure allows us to isolate the ENSO signal from the Interdecadal Pacific Oscillation.

Variables	**Definition**
Mixed Layer Depth (MLD)	Average depth at which the density changes from the surface is 0.125, in the box of Figure 1.
Net Heat Flux (NHF)	Sum of the latent, sensible, shortwave and longwave radiative fluxes average in the box of Figure 1
Sea Surface Temperature (SST)	Area average of SST in the box of Figure 1
Upwelling index (UI)	Zonal Ekman mass transport average in the box of Figure 1
Thermocline Depth (THD)	Depth of the 18ºC isotherm average in the box of Figure 1

Table 1: List of the variables used throughout the study to characterize the upwelling variability in the SCU region

Running mean of the unfiltered detrended fields are calculated to identify the evolution background mean state of the analyzed variables over time. The long term means of the analyzed period has been subtracted to each 20-year window mean to analyze the long-term variability.

Running ratio of variance and running correlations are applied to the filtered data in order to understand modulations in interannual variability and changes in the relation to ENSO.

We use a 20-year window, in accordance with the methodology of previous works (Rodríguez-Fonseca et al., 2009; Losada et al., 2012; López-Parages and Rodríguez-Fonseca et al., 2011; Martín-Rey et al., 2018). Regression and correlation maps are also computed for analyzing the related global oceanic and atmospheric conditions. To characterize ENSO, we use the Niño3.4 SST index downloaded from the NOAA website (https://www.esrl.noaa.gov/psd/gcos_wgsp/Timeseries/Nino34/), which is based on the SST anomalies averaged in the Niño3.4 region [150°W-90°W; 5°N-5°S] from HadISST dataset (Rayner et al., 2003). As for the SCU region, seasonal to interannual filters have been applied to the Niño3.4 index.

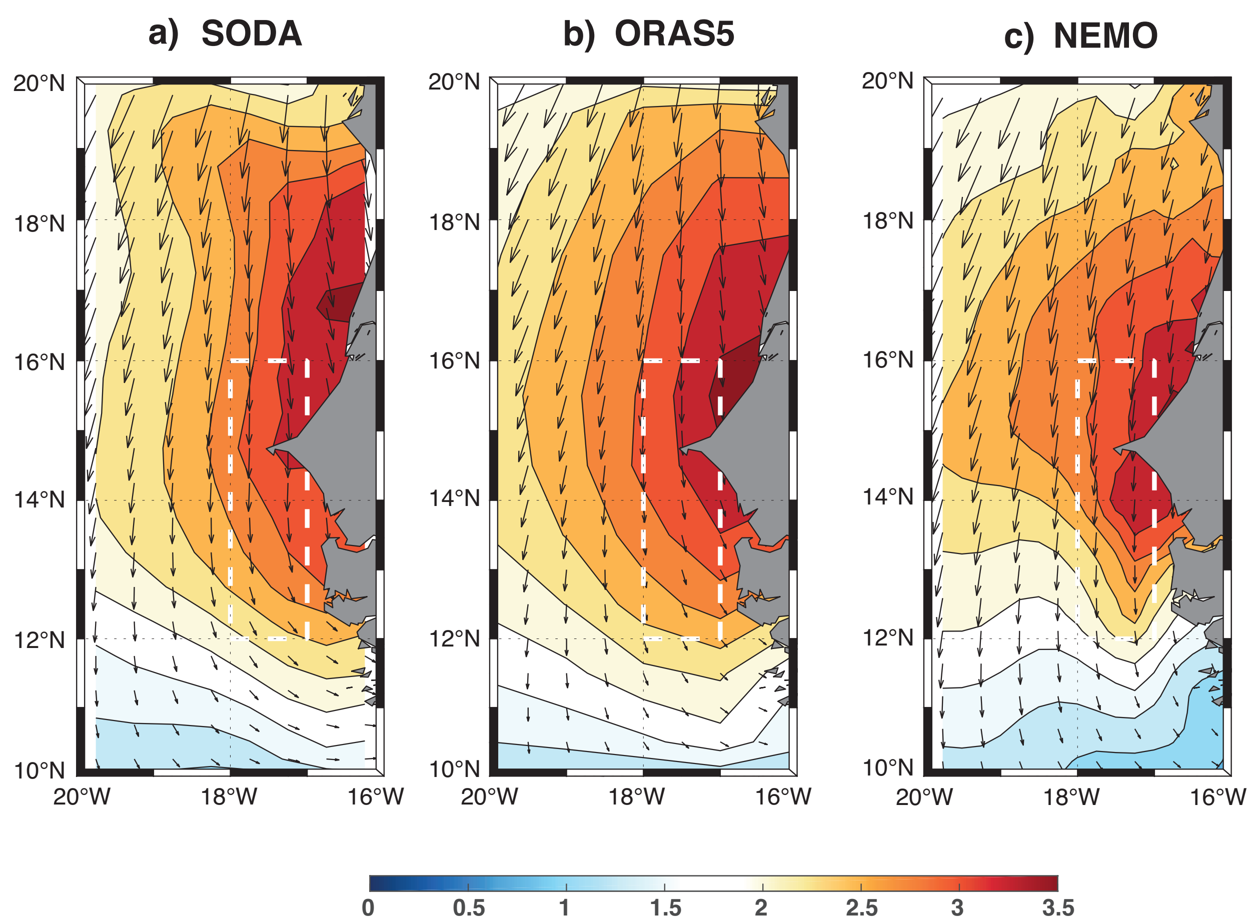

Figure 1: Region of Study. Annual standard deviation of SST (shaded) and annual mean of wind stress (arrows). Data comes from SODA reanalysis (a), ORAS5 (b) and NEMO simulation (c). The white dashed box indicates the area of study (SCU) used to compute the local environmental indexes. Period 1960-2008.

Finally, the statistical significance is assessed using different tests. For the ratio of variances and difference of means, we use an F-test and a t-test, respectively, with 95% of confidence. For correlations, a Bootstrap procedure (Monte Carlo technique with 500 permutations) is applied. Only those results that are significant at the 95% level are shown in the present study.

3 Results

3.1 Seasonal cycle of the local atmospheric and oceanic variables

All datasets reproduce a marked seasonal cycle for the different environmental variables considered in the area of study during the common period 1960-2008 (Fig. 2). Trade winds appear intensified in the SCU from January to April, and drastically weakened in boreal summer, in relation to the development of the West African Monsoon (Fig2. F, g). Consequently, the upwelling (UI) is considerably enhanced during late winter and tends to be canceled during the summer season (Fig. 2a,b). The thermocline depth exhibits a strong seasonal cycle, becoming shallower (deeper) in boreal winter (summer) in response to the upwelling cycle (Fig2.d), which is maximum in FMA. The mixed layer depth (MLD) is thicker during the boreal winter when stronger winds and densest surface waters enhance mixing depth (Fig2.b). Despite the robust agreement in the simulation of the oceanic seasonal cycle, discrepancies are found in the annual evolution of the net heat fluxes (Fig. 2e). Both ORAS5 and NEMOINT exhibit strong net heat fluxes from February to August, becoming weaker in autumn (black and blue lines). However, air-sea fluxes in SODA show a large contribution from January to April and are drastically reduced in summer months (red line, Fig. 2e). This inconsistency may be due to the use of the ensemble mean atmospheric fields from 20CRv2 reanalysis to force the ocean model. It averages out the high-frequency wind stress variability during periods with sparse observations (Giese et al., 2016), a persistent problem in some areas of the Tropical Atlantic basin.

All atmospheric and oceanic components illustrate large variability during the boreal winter in SCU region (Fig 2). Notice that wind stress and net heat fluxes of SODA present a maximum during the summer months (Fig. 2o-r), also reflected in the upwelling index and thermocline depth (Fig2 a,d-h). This may also respond to the above-mentioned bias associated with the choice of using ensemble mean atmospheric forcings. Using SODA3.4.2, this maximum disappears (see Figure Sx in additional material). Although these are issues involved in the representation of the seasonal cycle and the variability of SODA, air-sea fluxes should be taken into account in the interpretation of the results. In the present study, we focus on the upwelling season (FMA), where all data sets show fewer discrepancies.

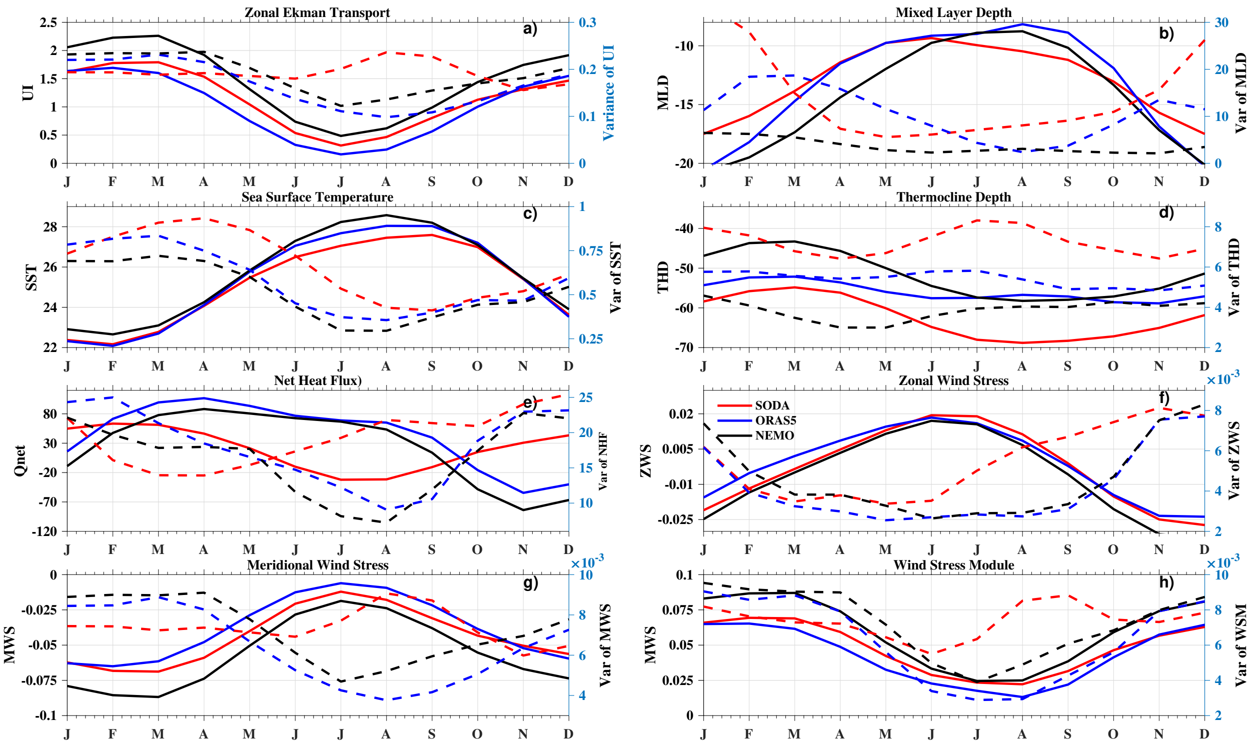

Figure 2: Seasonal cycle of the mixed layer heat budget terms. The seasonal cycle of mean (solid lines and variability (dashed lines) for the different components of the heat budget over the SCU region (region in Fig 1) and the period common to all: 1960-2008. Units are: for zonal Ekman transport and W/m^{2,} MLD and thermocline depth in m, and SST in SCU in ºC.

3.2 Changes in the interannual variability of the local atmospheric and oceanic variables

In this section we explore the modulation of the interannual variability by means of the evolution of the ratio of variance in each of the 20-year windows with respect to the variance of the common period (1960-2008). We calculate this ratio of variance for the different variables that characterize the mixed layer heat budget during the upwelling season (FMA). All atmospheric and oceanic variables show changes in the variability depending on the decades, highlighting a pronounced decadal modulation of the SCU interannual variability (Fig. 3).

All datasets reproduce a concomitant and statistically significant enhancement of the SST and UI variability in the 1960-1980 period and a substantial weakening from the 1990s onwards (black and grey lines, Fig.3). This common behavior suggests the existence of a dynamical coupling in the SCU region, which means that the SST variability is intimately linked to the upwelling variations before the 1980s. Nevertheless, the inter-decadal fluctuations in MLD, THD and Qnet differ among datasets. Slightly negative variations are found in SODA for the entire period (Fig. 3a), while ORAS5 and NEMO exhibit a positive tendency, with an increased significant THD and MLD variability from the late 1960s (red and green lines, Fig3b-c). Interestingly, Qnet variability changes also follow the SST and UI fluctuations throughout the period of study in NEMO and exhibit a significant increase around the 1970s for ORAS5 (blue line, Fig. 3b-c). In all variables, the loss of significance appears during the late 1970's, delimitated by a vertical line (Fig. 3a). This loss of significance starts in the 1976/77, coinciding with climate shift in the Indian (Nitta and Yamada 1989; Terray 1994; Aoki 2003) and Pacific (Nitta and Yamada 1989; Trenberth and Hurrell 1994; Graham 1994; Guilderson and Schrag 1998) oceans and could have an impact on remote teleconnections with SCU region.

The robust agreement in the SST and UI decadal behavior of the variability among datasets suggests the activation of a dynamical mechanism during the 1960-1980 period, which may be in response to local or remote forcings. Previous studies have reported interdecadal changes in the Tropical Atlantic Variability and its climate teleconnections (Foltz et al., 2019), associated with changes in the ocean background state or as part of inter-basin linkages between interannual modes; i.e., El Niño-Southern Oscillation ENSO, (Suárez-Moreno et al., 2018; Losada et al., 2012; Rodríguez-Fonseca et al., 2011, 2015; Dieppois et al., 2015; Martín-Rey et al., 2018).

However, the interannual to interdecadal variability of the SCU region, the underlying air-sea processes and its local and remote drivers have not so far been explored. Thus, the aim of the following section is to determine the mechanisms responsible for generating the interannual variability in the SCU region as well as their decadal variations. We will investigate the different contributions of the heat budget to SST variability during the upwelling season (FMA) and clarify the periods in which upwelling dominates.

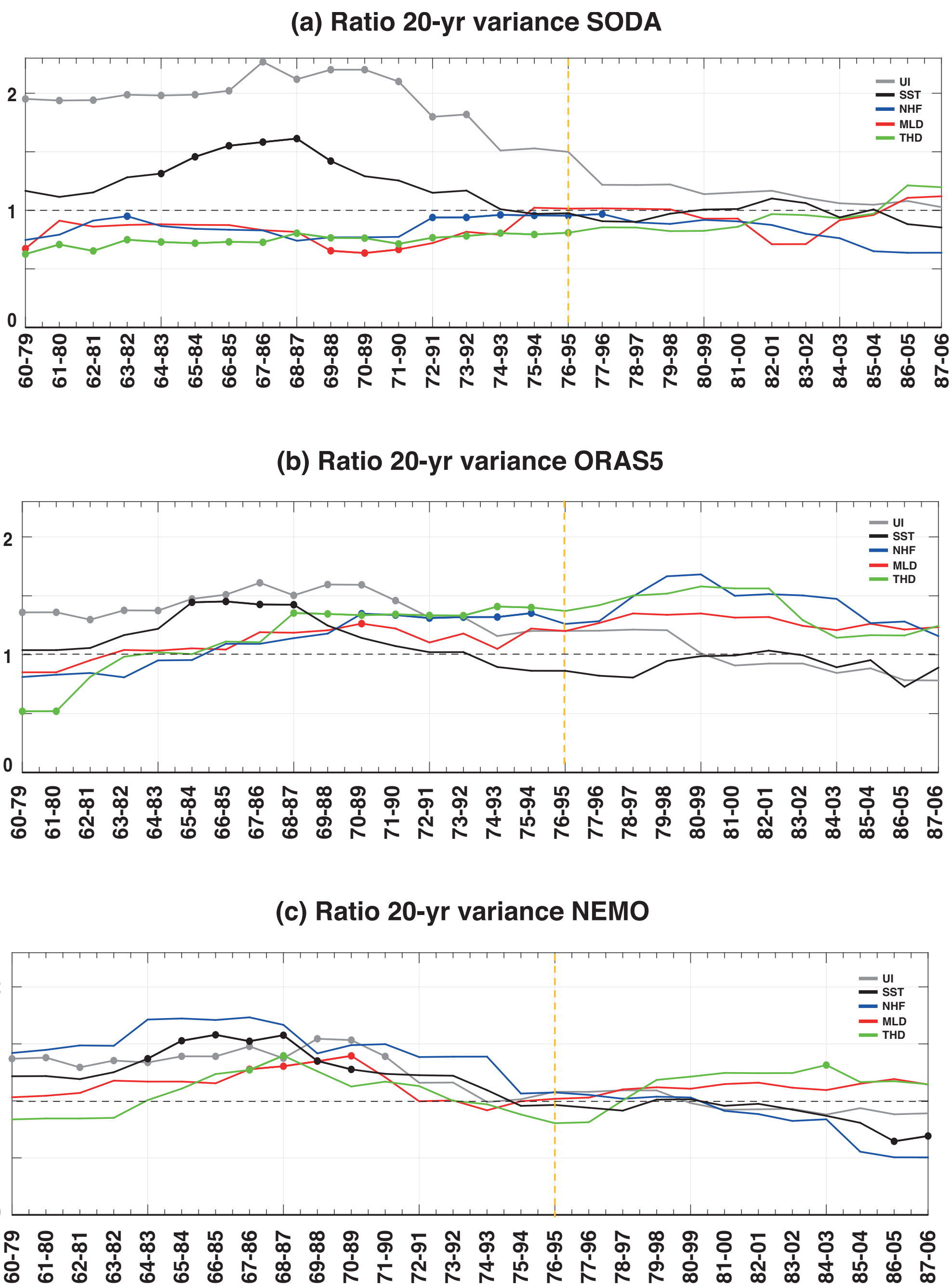

Figure 3: **Evolution of the Mixed Layer Heat Budget Terms Variability.** The time-evolution of the FMA 20-year window ratio of variance computed for the mixed layer heat budget variables averaged in the SCU region [18°W-17°W and 12°N-16°N] for (a) SODA reanalysis, (b) ORAS-5 reanalysis and (c) NEMO-INT simulation. For each window, the variance is calculated and compared to the reference period 1960-2008. Dots indicate the statistically significant changes at a 95 % confidence level according to an F-test. The orange vertical dashed line is highlighted to separate those periods with different behaviors.

3.3 Non-stationary drivers to the local SST variability

To assess the role of the different physical drivers behind the decadal changes undergone by the local SST variability throughout the study period (Fig. 3), we compute the 20-year running correlations between the anomalous local SSTs and the local atmospheric and oceanic variables contributing to the mixed layer heat budget (Fig. 4).

At first sight, we already observe a marked shift in the linkage between the local SST and the different components of the heat budget (Fig. 4a-c). The mixed layer depth (red line) and the upwelling index (grey line) are significantly correlated with SCU SSTs throughout the first half of the period of study (1960s-1980s). Positive correlations with the MLD (red line) mean that the deeper (shallower) mixed layer depth is related to positive (negative) SST anomalies. Negative correlation with UI means that strong westward Ekman transport is associated with a sea surface cooling (negative SST anomalies). In contrast, the relationship between thermocline depth and the local SST becomes stronger and significant from the 1990s (green line, Fig. 4a-c). Notice that the correlation between net heat fluxes (NHF) and SST changes tends to negative (insignificant) values throughout the record, which suggests a damping effect on the SST signal. It is worth pointing out that our results highlight the activation of different local drivers contributing to the SST interannual variability throughout the observational record. During the 1960-1980 period, dynamical mechanisms involving the coastal upwelling (zonal Ekman transport) control the SST variability. From the 1980s onwards, the dynamical contribution is reduced, becoming insignificant, while the NHF still illustrates a damping contribution. The consistent behavior in all datasets shows that other mechanisms start to drive the SCU SST variability in the 1980-2000 period. However, it is pertinent to ask what the causes for this alternating behavior are. For example, is the contribution of the thermodynamic/dynamic processes influenced by changes in the background conditions?

The shift in the local SST drivers is consistent with the changes in the running standard deviation, mainly in relation to SST and upwelling (Fig. 3). Thus, the higher the variability of SST and upwelling, the stronger the relation between SSTs and MLD and UI (Fig4 a-c), while the decrease in variability after the 1980s coincides with a reduction in the impact of upwelling in SST.

We also investigate the role of the changes in the mean of the mixed layer heat budget components and the association with changes in the local SST drivers (Fig 4d-f). These decadal variations should be interpreted as the changing background conditions under which the aforementioned non-stationary interannual links with SST variability occur. To simplify the analysis, we select 2 periods based on the role of zonal Ekman transport on SST. In the 1960-1980 period (hereafter denoted as P1, Period “1”), the stronger mean Ekman transport (grey line, Fig. 4 d-f) acts under a shallower mean thermocline (green line, Fig. 4d-f) and a cooler sea surface (black lines, Fig. 4 d-f). During the 1990-2000 period (hereafter denoted as P2, Period “2”), the THD becomes deeper and the mean Ekman transport is significantly reduced (grey and green lines, Fig. 4 d-f). These decadal subsurface changes agree with a SCU region more sensitive to external perturbations in P1 than in P2 (Martín-Rey et al., 2018).

ORAS, NEMO and SODA present a similar evolution of the 21yr changes in the SCU mean state. The common features suggest a shallower mean thermocline in P1, with colder SSTs and enhancement of the westward zonal Ekman transport (Fig. 4 d-f), which together with enhanced upwelling and SST variance (Fig.3a-c) may account for the dominant role played by the dynamical processes (Ekman transport) in controlling the local SST variability (Fig. 4a-c). On the other hand, the background state in P2 becomes unfavorable, with a weaker mean Ekman transport and a deeper mean thermocline, also reflected in a drastic diminution of SST and upwelling variance (Fig. 3a-c), which may reduce the effectiveness of the dynamic drivers in generating the local SST variability (Fig. 4a-c). Notice that for SODA, we have added the analysis of the SST physical drivers using the v.4.3.2 version. The agreement using this database confirms the use of SODA v.2.2.4 for analyzing the drivers.

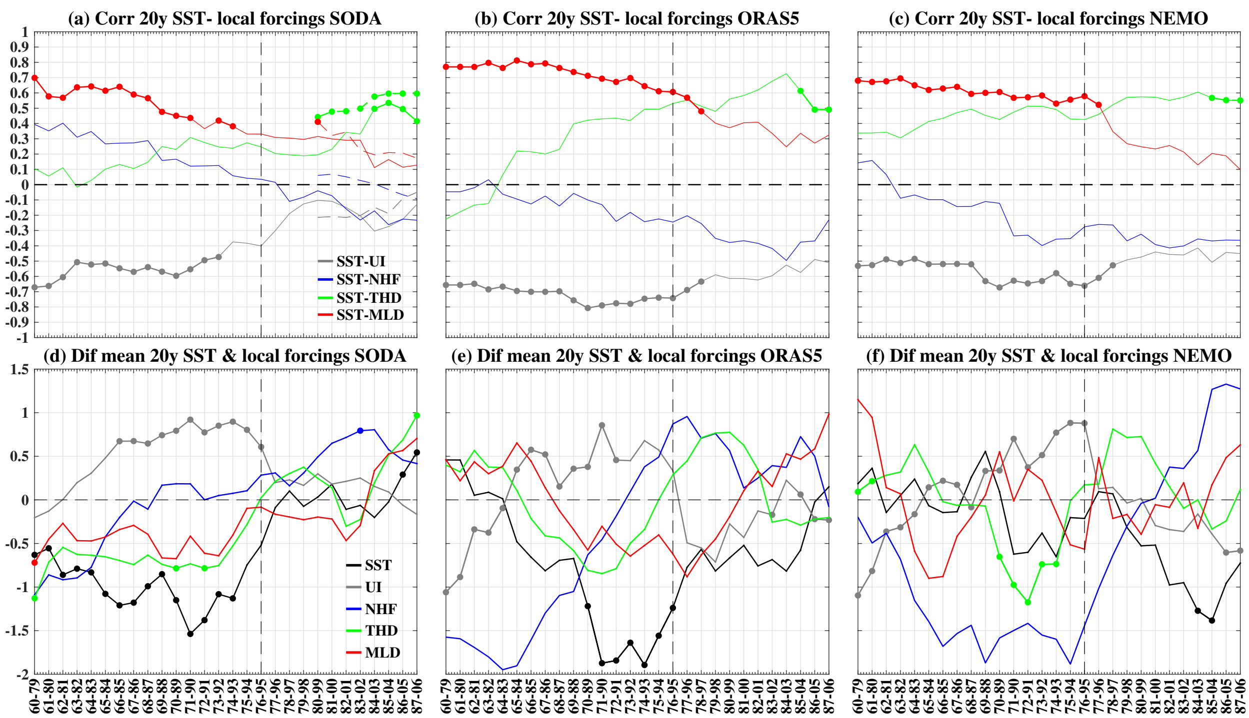

Figure 4: (a-c) <u>Evolution of local SST interannual variability drivers.</u> The time-evolution of the 20-year window running correlation between local interannual SST variability and the physical variables contributing to the mixed layer heat budget for(a) SODA reanalysis for the period 1900-2008 (the discontinuous lines at the end of the records in (a) are calculated with the SODA v3.4.2), (b) ORAS-5 reanalysis and (c) NEMO-INT simulation for the period 1960-2008. Dots indicate 95% significance values using a Monte Carlo test (500 simulations)**. (d-f) <u>Mean state conditions.</u>** Time-evolution of the 20-year window running mean of the detrended but unfiltered data from different physical variables contributing to the mixed layer heat budget with respect to the mean for the total period 1960-2008 for (d) SODA reanalysis, (e) ORAS-5 reanalysis and (f) NEMO-INT simulation. Positive values of MLD and THD indicate deepening and vice versa for negative values. Dots indicate the statistically significant changes at a 95 % confidence level according to a T-test.

It is interesting to note that during P2 the mean and variance of the zonal Ekman transport become drastically weaker (Fig. 3a-c and Fig. 4d-f). At the same time, the contribution of the net heat fluxes gradually gains weight (blue lines, Fig.4d-f). At interannual time scales, it translates into a stronger damping effect of net heat fluxes on the SCU SST variability (blue line, Fig 4a-c). This, together with the inactive upwelling influence in P2 (grey lines, Fig 4a-c), brings to light the significant contribution of additional mechanisms to generating local SST variability. In this sense, horizontal advection may play a dominant role in the SCU during P2 (Faye et al, 2015). However, the analysis of this contribution is beyond the scope of this study.

Our results demonstrate for the first time that the drivers of the SCU SST variability change throughout the observational record, which shows an activation/deactivation of the dynamic (upwelling) local mechanisms coinciding with a modification of the background state.

The favorable/unfavorable mean conditions may affect not only the activation of these processes of diverse nature, but also the effectiveness of remotely forced teleconnections. In particular, the ENSO impact on the North Tropical Atlantic SST variability, which is known to be positive (El Niño with warm TNA conditions and La Niña with cold TNA conditions) and stationary in the boreal spring (Enfield and Mayer 1997; García-Serrano et al., 2017), may be different in the SCU, depending on the background mean ocean conditions (Martín-Rey et al. 2018). The impact of ENSO on the Eastern North Tropical Atlantic and its stationarity on time has not been investigated in depth. In the following section, the impact of ENSO on the SST variability at the coastal upwelling off the Senegalese coast is analyzed.

3.4 ENSO as a non-stationary forcing of SST variability in the SCU region

In the previous section, we have provided robust evidence regarding the different processes controlling the SST variability in our study region, depending on the period of study. This non-stationary behavior may be due to the existence of different drivers that alter the variability of local winds, and thus, of the SCU SST. Several studies point to the significant role of ENSO in generating SST responses in the Tropical North Atlantic (Okumura and Xie,2006; Wang,2006; García-Serrano et al., 2017), and how ENSO teleconnection varies from some decades to the others, due partially to the low-frequency variability of the Atlantic and Pacific Oceans (Mariotti et al., 2002; López-Parages and Rodríguez-Fonseca 2012; López-Parages et al., 2015, 2016; Martín-Rey et al., 2018). Moreover, decadal variations in the ocean background state may either favor or inhibit the impact of remote forcings (Martín-Rey et al., 2018), which in our region may modify the related anomalous SST response over the SCU. Thus, both atmospheric and oceanic conditions may play a fundamental role in whether or not the ENSO impact on the study region is enhanced.

In order to investigate this issue in greater depth, we calculate the evolution of the 20-year window running correlation analysis between the Niño3.4 SST index and the anomalous environmental local variables off Senegal (Fig. 5).

The correlation between ENSO and the local SST variability occurs throughout almost the whole period (Fig 5. Purple line) but not for the same reasons.

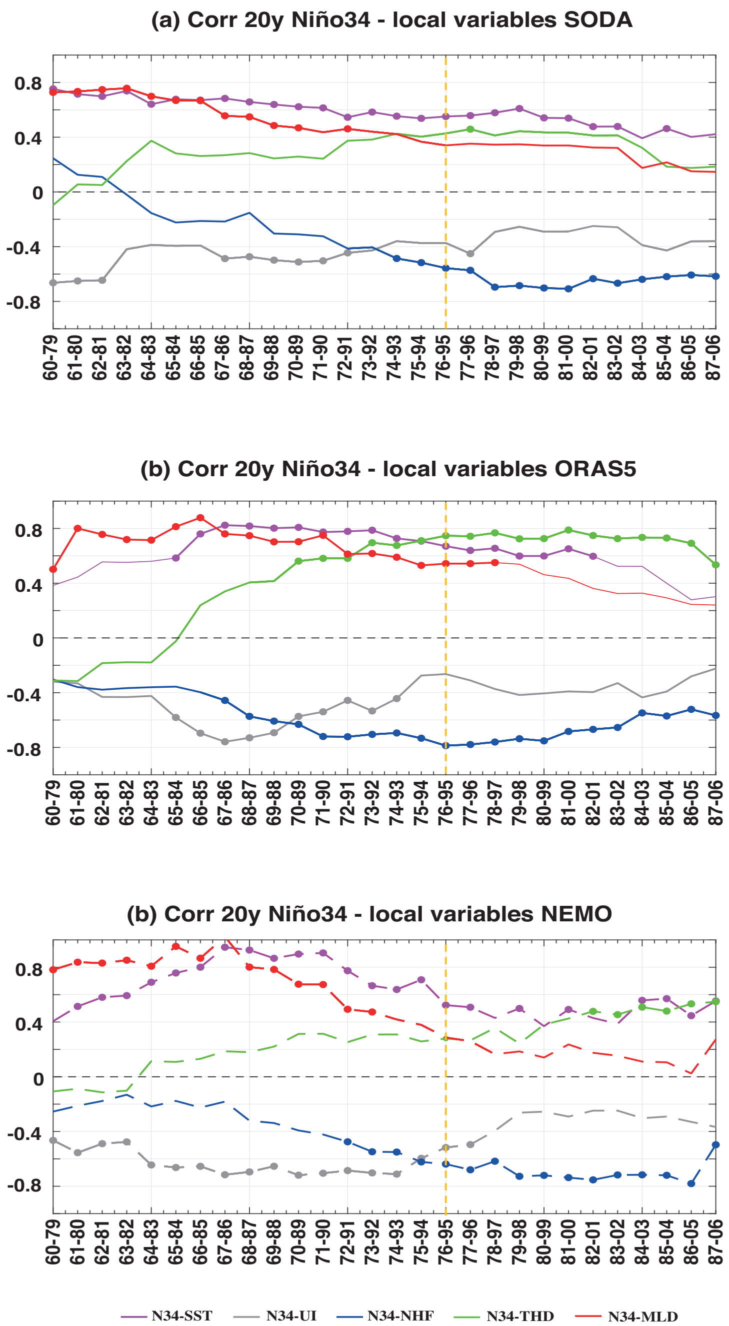

Figure 5: <u>ENSO impact on local SSTs & Mixed Layer heat budget components.</u> The time-evolution of the 20-year window running correlation between the Niño3.4 index and local physical variables contributing to the mixed layer heat budget at interannual timescales for: **(a)** SODA. **(b)** ORAS5 and (c) NEMO-INT simulation respectively for the period 1960-2008. Dots indicate the 95% significant values using a Monte Carlo test (500 permutations).

Significant correlations between ENSO, the local upwelling index and MLD are only found in P1 (Fig. 5), which is in agreement with the correlation between local SST and upwelling (Fig 4a-c). In contrast, in P2, a significant link exists between ENSO and thermocline depth (green line) and Qnet (solid blue line). Nevertheless, the sign of the correlation reveals that ENSO-induced Qnet has a damping effect on the local SST anomalies. This, together with the weakening of the ENSO-induced upwelling (grey lines) may be partially responsible for the slight reduction in the linkage between ENSO and SCU SSTs (pink lines, Fig. 5). This relation is consistent among all databases.

Our results show that the ENSO teleconnection to local SSTs occurs by altering the Ekman transport during some periods (1960s-1980s), a feature that seems to be particularly sensitive to the background conditions of the UI and THD. Only in those periods in which the thermocline depth is shallower than usual and the upwelling contribution is reinforced (see green and grey lines in Fig. 4d-f), do the SCU regions become more receptive (enhanced variance) to external forcing (see green and grey lines in Fig. 3), having ENSO a significant influence (Figure 6). However, when the mean thermocline depth is deeper (during P2; see Fig. 4 d-f), ENSO has a lower and insignificant effect on the upwelling, and a weaker influence on the local SST variability (grey and magenta lines, Fig. 5, maps in Fig.7).

It is worth mentioning that during the most recent decades (from the 1980's onwards; i.e. "P2"), while the ENSO influence on local SSTs is reduced, it is still significant (magenta lines, Fig. 5). This suggests that the active dominant processes for the SCU SST variability are different from those in "P1" (Fig. 5). During this more recent period, ENSO-upwelling linkage becomes weaker (see also Fig 8. Top-right panel) and the damping NHF effect is persistent in the study area (see also Fig 8. Bottom-right panel). Thus, the positive SST anomalies caused by El Niño (dashed magenta solid line, Fig. 5) during those decades (1980s to 2000s; i.e., "P2") may be generated by other processes, such as horizontal advection (Faye et al., 2015). This consistent shift among datasets in the local drivers of the SCU SST variability from the 1980s may substantiate the role of meridional and zonal advection mechanisms. However, this is beyond the scope of the present paper.

To illustrate more clearly the aforementioned non-stationary link between ENSO phenomenon and the SCU SSTs via the modification of local winds, we show the regression maps of the local SST index in FMA (averaged within the dashed square boxes shown in Fig. 1) onto the global SSTs and winds during the "P1" (Fig. 6), lagging SST and winds up to 4 months. These global maps are obtained separately for those periods in which the ENSO-SCU link appears active or inactive; that is, whether or not those periods in which the Niño3.4 index and the upwelling index are significantly correlated (grey line in Fig. 5); as expected, one may observe a coherent El Niño pattern (peaking in DJF) in "P1" (Fig. 6a-i). Notice that the large-scale forcings of local SCU SSTs are coherent in all datasets, giving robustness to the non-stationary role of ENSO in modulating the North West African upwelling variability.

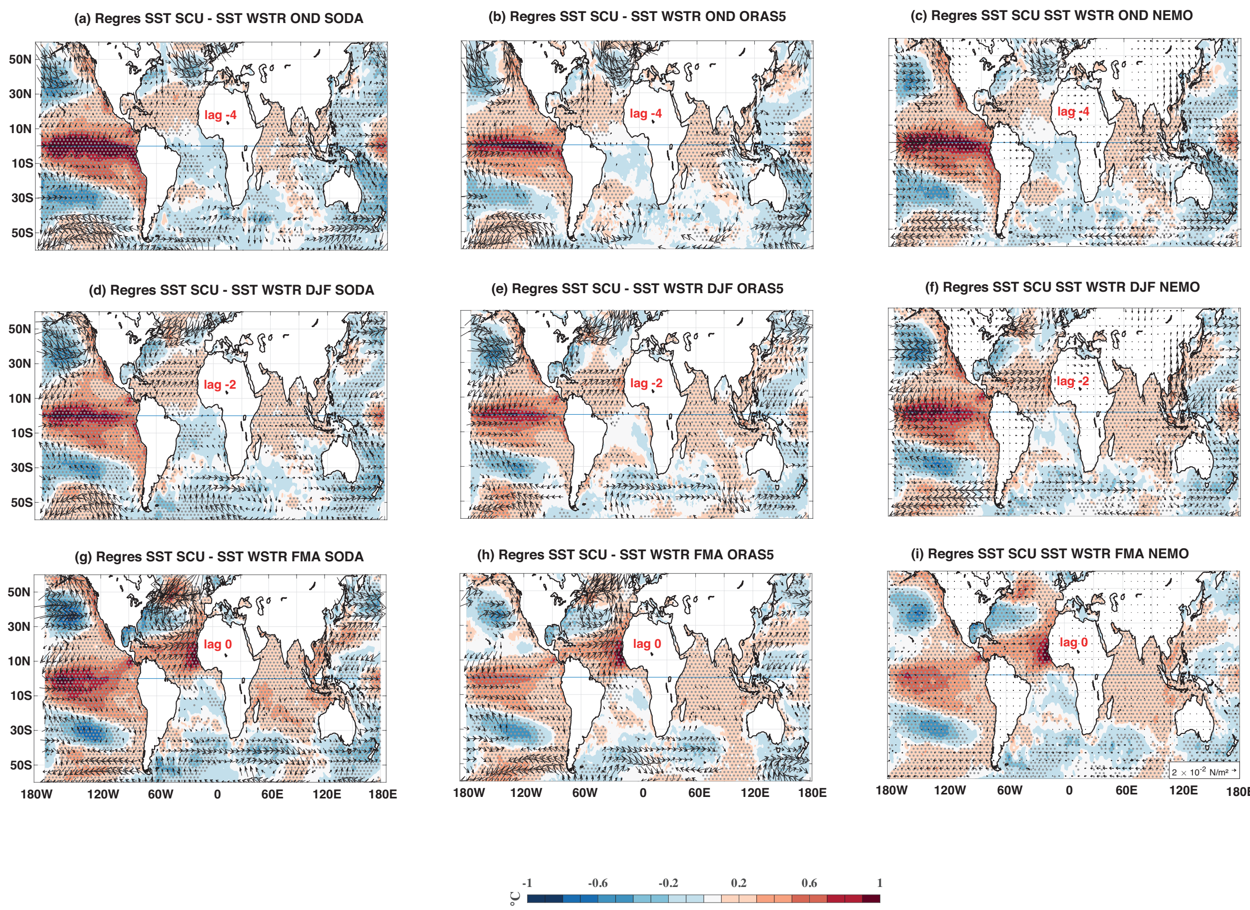

Figure 6: **Spatial structure of the teleconnection for P1 period 1961-1990.** Regression maps of the local standardized SST index in FMA (averaged over the box defined in Fig. 1 and filtered at interannual timescales onto global SST (shaded, °C) and wind stress (vectors, N/m²) over the ocean, from lag 0 to lag -4 months, during the period with significant ENSO impact (1961-1990, or period "1"); for SODA (left panels), ORAS-5 (middle panels) and NEMO-INT (right panels). Statistically significant areas are stippled (grey dots) and black vectors indicate wind speed significant at the 95% level using the Monte Carlo test (500 permutations of the original time-series).

A tripole pattern of SST anomalies is identified in the North Atlantic, which resembles the well-known SST fingerprint associated with the NAO (Sutton et al., 2000). These SST anomalies appear particularly intense over the eastern TNA (that is, off the African coast) due to the weakened trade winds (Fig. 6d-i). In fact, The NAO can be forced by ENSO and, in turn, produces the SST tripole which can have an impact on upwelling. Indeed, upwelling index regression map onto SSTs resembles a clear ENSO pattern (Fig8-9-10. Top-left panel). Over the North Pacific region, there is also a structure in the SST anomalies resembling the impact of the PNA pattern on the ocean, which is also characterized by a weakening of the trades due to the weakening of the subtropical high-pressure system (Fig. 6d-i).

In contrast, during period 2 (from 1990s onwards), when ENSO exert a weaker impact on the SCU region, a tripole-like pattern appears over the North Atlantic during the upwelling season (Fig 7g-i). Nevertheless, this signal is not persistent and low correlation values are obtained with upwelling (Fig 8-9-10., Top-right panel).

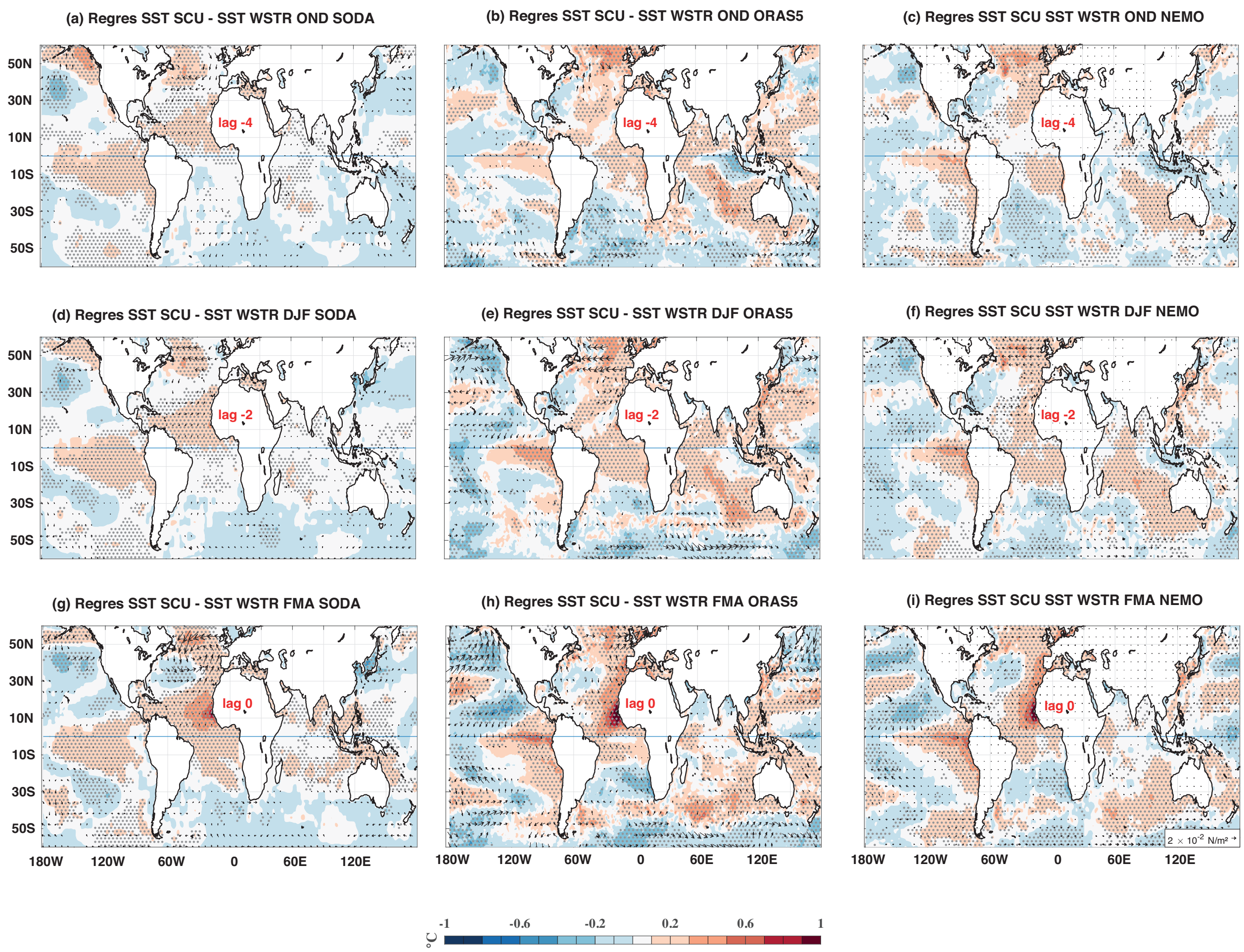

Figure 7: **Spatial structure of the teleconnection for P2 period: 1991-2008**. Regression maps of the local standardized SST index in FMA (averaged over the box defined in Fig. 1 and filtered at interannual timescales) onto global SST (shaded, °C) and wind stress (vectors, N/m²), from lag 0 to lag -4 months, during the period with no Niño impact (1991-2008) for SODA (left panels), ORAS-5 (middle panels) and NEMO-INT (right panels). Statistically significant areas are stippled (gray dots) and black vectors indicate wind stress significant at the 95% level using the Monte Carlo technique (500 permutations of the original time-series).

To illustrate these results more clearly, we also quantify the relative importance of thermodynamic vs. dynamical processes in determining the amplitude of SST variability. Figures 8- 9-10 represent the result of regressing the upwelling Index (UI) and the Net Heat Flux onto the global SSTs and winds for the 2 different periods as well as the different data bases. Comparable results are found between the regression of the local SST index (Figures 6 and 7) and the UI onto global SST. Regression values associated with Net Heat Flux are very weak, which suggests that dynamical processes are more at play than thermodynamical processes.

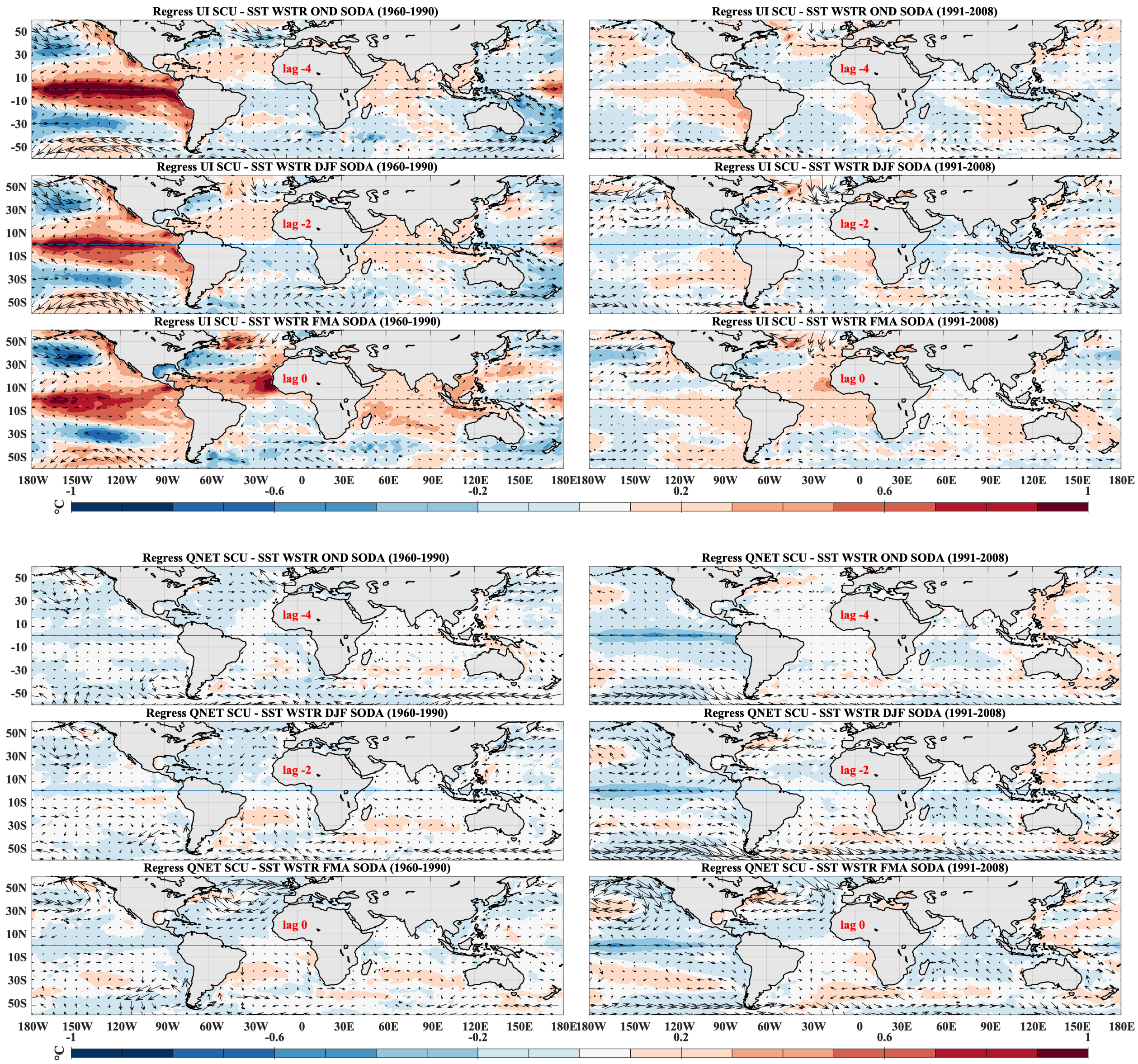

Figure 8: As in Figures 6 and 7, but regressing the upwelling index (top panel) and the Net heat flux index (bottom panel) onto global SSTs for the 1960-1990 period (left columns in each panel) and the 1991-2008 period (right columns in each panel). UI and Net heat flux indices come from SODA2.2.4

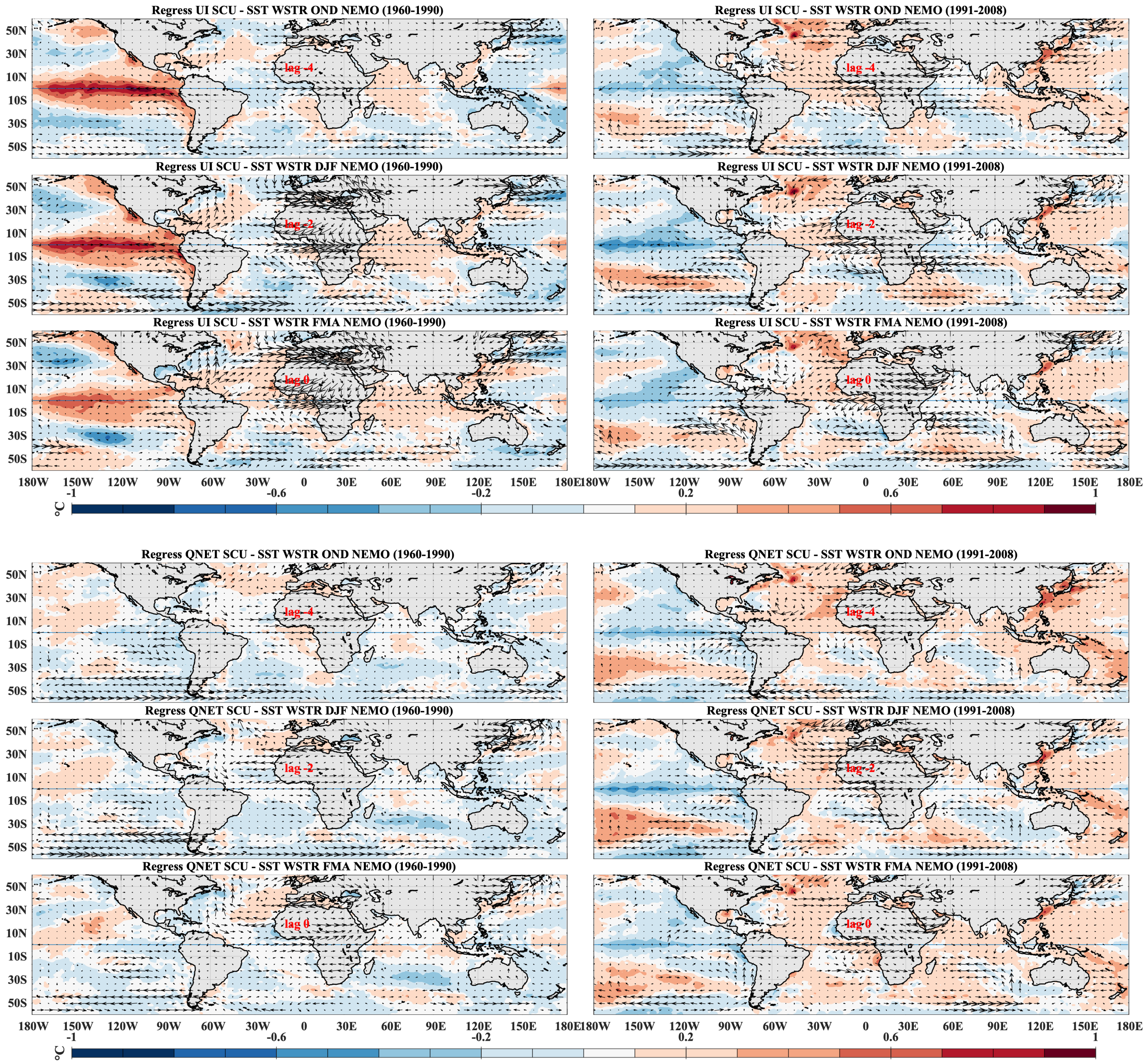

Figure 9: As in Figure 8, but UI and Net heat flux indices come from NEMO simulation

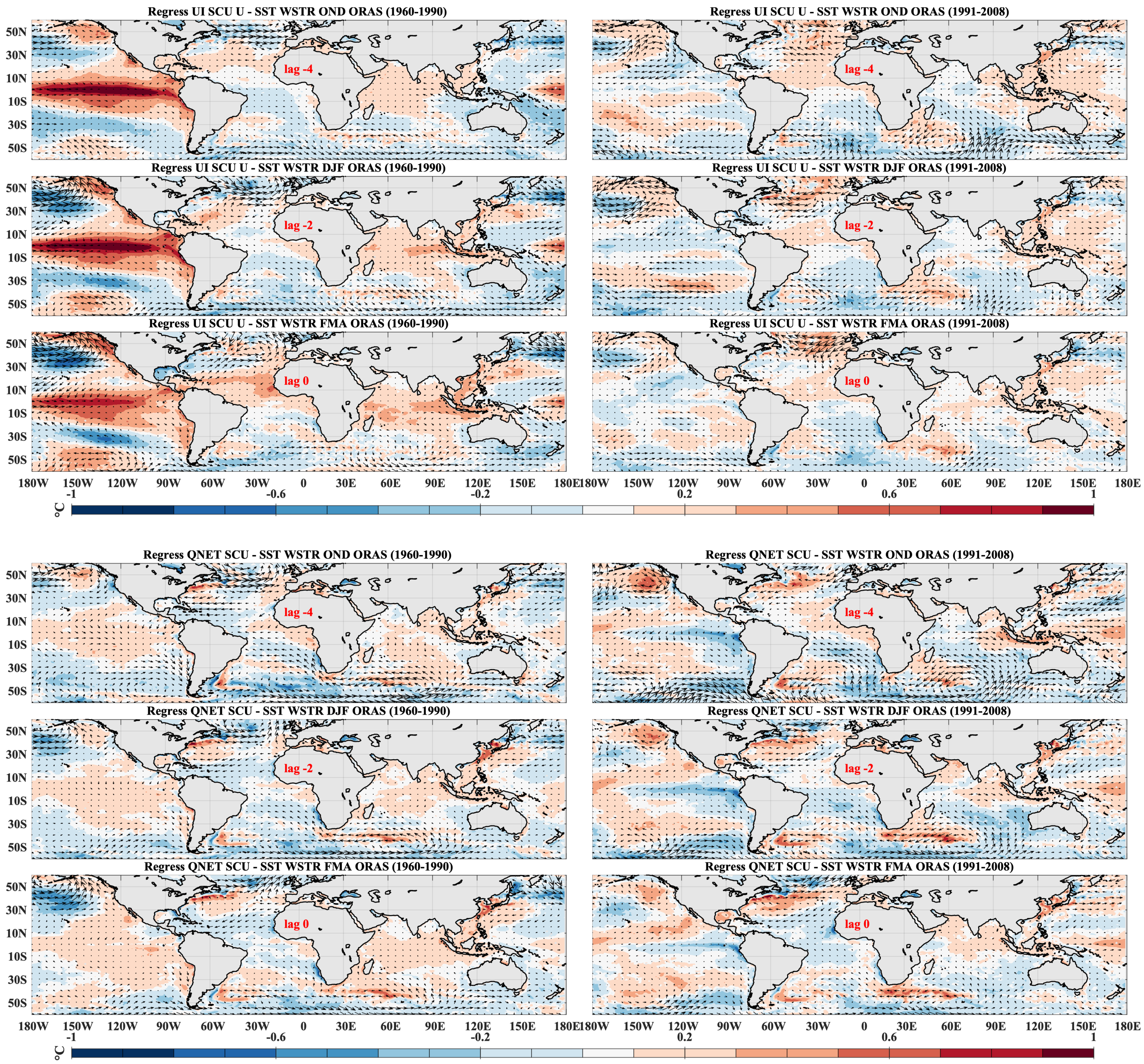

Figure 10: As in Figures 8 and 9, but UI and Net heat flux indices come from ORAS5.

3.5 The modulating role of the background state

In previous sections, we have provided robust evidence about the varying contribution of dynamical processes on the SCU SST interannual variability, depending on the decades considered. Furthermore, the switch on/off for the dynamic contribution seems to be strongly linked to changes in the ocean background state, thereby affecting the ENSO impact on the SCU upwelling.

In order to explore further the interdecadal variability of the ENSO impact on SCU SSTs, we calculate20-year correlations between Niño3.4 and local SST drivers on the longer available record of SODA reanalysis, from 1901 onwards (Fig. 11, which is an extension of Fig 5.a). A surprising result emerges that brings to light a pronounced multidecadal variability in the ENSO impact on local SSTs and associated drivers. A clear non-stationary link between the ENSO and the SCU SST is identified, significant correlations from the 1900s to the 1930s and from the 1960s to the 2000s being found, while correlations tend to zero for the years in between (1940s and 1950s, magenta solid line, Fig.11). As an initial attempt to identify the modulator behind this change in the West African SST variability and its role in ENSO-SCU teleconnection, a regression map of the Niño3.4-upwelling correlation curve (grey line in Fig. 11.a), filtered at decadal time scales onto global SSTs, and wind stress for the whole period is performed. The resultant global pattern (Fig. 11.b) is characterized by a pan-Atlantic warming in the northern hemisphere resembling an AMV-like SST structure in its positive phase (Knight et al., 2006). An anomalous warming over the North Atlantic region is accompanied by weakened easterly winds and positive SST anomalies over the SCU area (Fig. 11b).

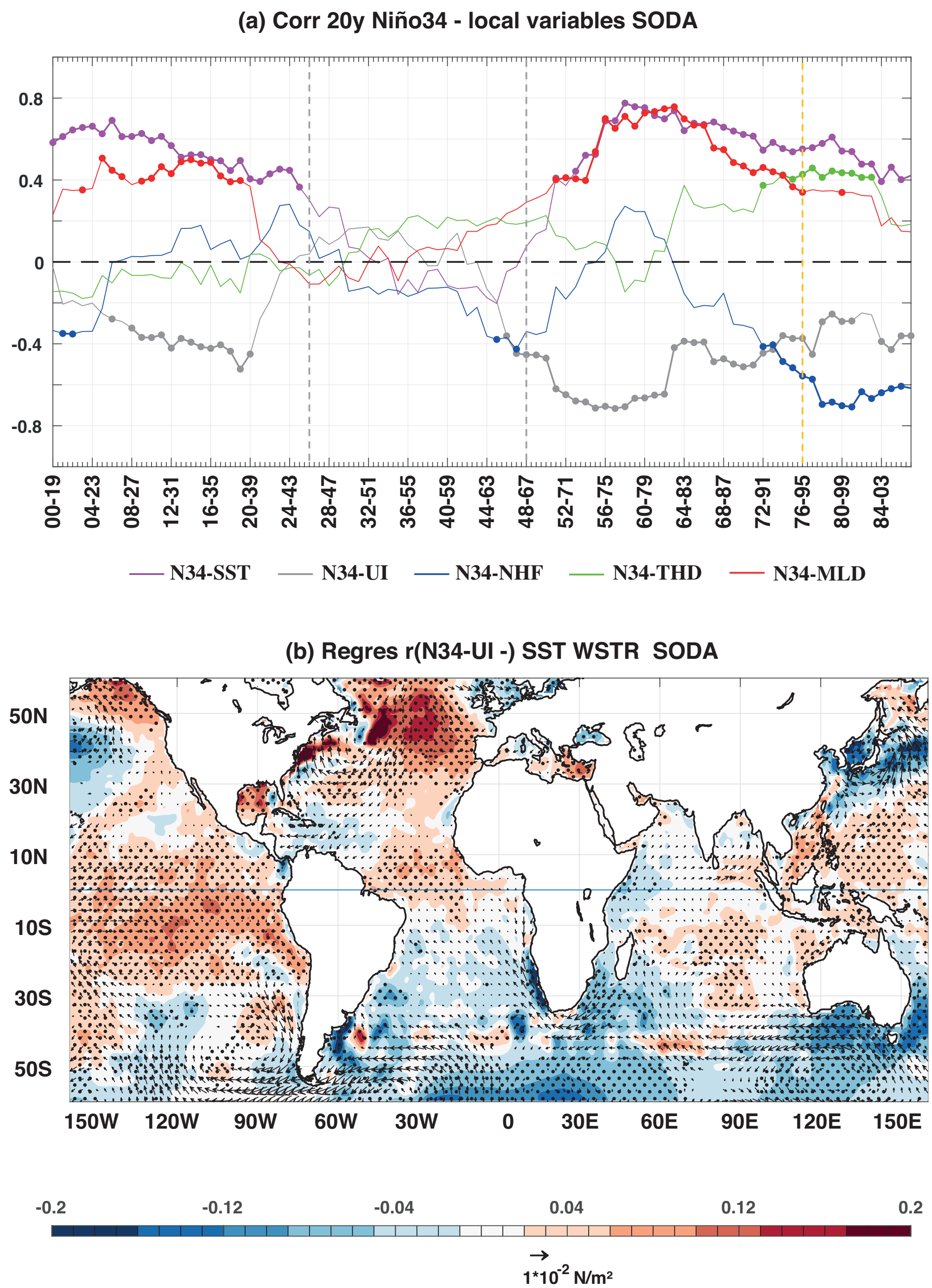

Figure 11: **Modulation of the change in ENSO impact on upwelling.** Winter lagged regression map of the Niño Upwelling correlation index (grey line, Fig. 5a) onto global SST (Shaded, °C) and wind stress (vectors, N/m²) during the period 1901-2008. Statistically significant areas are stippled (black dots) and only significant wind stress are shown (black vectors) using the Monte Carlo technique (500 permutations of the original time-series).

In this global background state, and following the evolution of the correlation curve (grey line in Fig. 11-a), no teleconnection between anomalous local Ekman transport and ENSO takes place. The opposite occurs when the correlation is negative, indicating that during decades in which the North Atlantic is colder than the South Atlantic (negative AMV), ENSO teleconnection over the upwelling in the SCU region is stronger. Thus, it seems that the evolution of the correlation curve evolves in phase with the evolution of AMV (Knight et al., 2006). On the one hand, it has been reported how ENSO variability and its flavor changed in phase with AMV (Trascasa-Castro et al., 2021; Yu et al, 2015), impacting its teleconnections. But, on the other hand, here we have found how the background state of the Atlantic Ocean also changes, being more or less receptive to external forcings coming from ENSO.

Based on previous research done by several authors, different causes may be inferred: the AMO may first modulate the effectiveness of the atmospheric ENSO-SCU teleconnection through changes in the global atmospheric mean state (López-Parages and Rodríguez-Fonseca, 2012; Zhang et al., 2019). Secondly, negative AMO may set up the favorable local ocean background state: colder mean SSTs and shallower mean thermocline favor the impact of surface wind stress on upwelling (in agreement with Martín-Rey et al., 2018). All these factors could point to the Atlantic Multidecadal Variability (AMV) as an important modulator of the ENSO-SCU teleconnection analyzed here. This result is also coherent with previous findings from Martín-Rey et al. (2018), who stated that during negative AMV phases, the thermocline depth in the Eastern Tropical Atlantic is shallower, favoring the Bjerknes feedback and increasing the equatorial SST variability. In this scenario, the ocean dynamics are more active, generating new overlooked equatorial modes co-existing in the basin (Martín-Rey et al., 2018, 2019). In addition to these changes in the Atlantic background conditions, decadal variations in the remote forcings of the SCU variability, as in ENSO properties (Fedorov and Philander 2000; Dong et al., 2006; Levine et al., 2017), may also contribute to the non-stationary ENSO-SCU teleconnection. This aspect is however beyond the scope of the present study and should be further investigated in future works.

To summarize, our results suggest the influence of the AMV on the atmospheric ENSO-SCU teleconnection by changes in ocean background changes off Senegal. A realistic background state is crucial for better understanding the impact of ENSO on the SCU.

4. Conclusions

We use monthly data of SODA reanalysis v2.2.4, ORAS5-reanalysis and an interannual NEMO-INT simulation with prescribed air-sea fluxes to diagnose the variability of those physical processes that may alter the SSTs in the upwelling region located off the Senegalese coast (Cape Verde Peninsula region). All variables exhibit a strong seasonal cycle with a maximum variability of the upwelling in FMA. We then focus on the FMA season in order to analyze the role of the different physical variables on SST variability and how their mean state and variance change with time. We infer functional relationships between the SCU-SST and dynamic and thermodynamic variables, thereby detecting changes in the local drivers of SST associated with a modification of the background state. Two different regimes are found: one occurring during 1960s-1980s (period P1), and the other occurring afterwards during 1990-2008 (period P2). We found that the SCU upwelling in P1 is more sensitive to remote ENSO teleconnections than in P2. El Niño impact on upwelling is very weak in P2, in which the damping contribution of net heat fluxes to local SST variability is stronger than in P1. This suggests that ENSO teleconnection through additional processes (i.e., horizontal advection) is dominant from the 1990s, while Ekman-induced upwelling controls the local SST variability in P1. Using the whole SODA reanalysis covering the 20th century, we find a period in which neither the Ekman transport nor the surface heat fluxes are altered by ENSO and El Niño-local SST correlations are not significant (Fig. 11a). This is the case in the 1940-1950 period, when no impact of ENSO on local SSTs is found.

A mechanism is proposed for the different regimes found. In P1, the ocean is colder over the North Atlantic Ocean, and the winds and turbulent heat fluxes are stronger (Fig.6 and Fig.4c-d). The MLD and the thermocline are shallower, and thus dynamical processes (Ekman transport) control the interannual SCU SST variability. During these decades, the ENSO impact on upwelling becomes stronger, also impacting on MLD. In contrast, in P2 the ocean is warmer as a consequence of a deeper thermocline and weaker winds (Fig. 7 and Fig. 4c-d), since strong heating occurs due to turbulent heat fluxes. However, at interannual time scales, the turbulent thermodynamic forcing tends to damp the interannual SST variability. In addition, during these decades, a weaker impact of ENSO on the upwelling is found. Thus, other processes such as horizontal advection may control the SCU SSTs.

We demonstrate herein how the role of ENSO in the local SST variability is not stable throughout the observational record, and thus the role of the multidecadal variability of the ocean background needs to be explored. The mean global SST background state that favors the upwelling impact on SST variability resembles an AMV-like structure related to changes in the winds over the North Atlantic region. This finding suggests that the Atlantic Multidecadal Variability (AMV) may act as a modulator for the ENSO-SCU teleconnection. Nevertheless, sensitivity pacemaker experiments or anomaly coupled experiments should be designed to gain a better understanding of this change in the variability.

The results presented here have a substantial potential impact for seasonal predictability. Models are unable to represent neither ENSO associated teleconnections nor the multidecadal variability of the Atlantic correctly. One of the reasons could be associated with the inability to produce the correct background and mechanisms regarding the variability of the processes involved. One of the main findings of the present study highlights the role of decadal variability in the understanding of the interannual variability. This information may prove useful for the climate modeling community in its endeavors to achieve an improvement in simulations of ENSO associated teleconnections.

Acknowledgements:

The research leading to these results has received funding from the CSIC ICOOP projects: ICOOPB20204, ICOOPB20358 (the UCM Cooperation Project from XIV and XVII calls); the Spanish Project CGL2017- 86415-R;

the EU/FP7 PREFACE (Grant Agreement 603521) and TRIATLAS H2020 EU project (Grant Agreement 817578). The authors would like to thank Jean-Marc Molines for his invaluable assistance in conducting the simulations with the ATLTROP025 model. MMR received funding from the MSCA-IF-EF-ST FESTIVAL (H2020-EU project 797236) and from a *Juan de la Cierva* Incorporation (IJC2019-041150-I) research contract of MICINN (Spain). This work was also supported by the TRIATLAS project, which has received funding from the European Union's Horizon 2020 research and innovation program under grant agreement No 817578."

References

Aoki S (2003). Multidecadal warming of subsurface temperature in the Indian sector of the Southern Ocean. J Geophys Res 108:8081. https://doi.org/10.1029/2000JC000307

Alexander, M., & Scott, J. (2002). The influence of ENSO on air-sea interaction in the Atlantic. Geophysical Research Letters, 29(14), 46-1.

Amaya, D. J., & Foltz, G. R. (2014). Impacts of canonical and Modoki El Niño on tropical Atlantic SST. Journal of Geophysical Research: Oceans, 119(2), 777-789.

Amaya, D. J., DeFlorio, M. J., Miller, A. J., &Xie, S. P. (2017). WES feedback and the Atlantic Meridional Mode: observations and CMIP5 comparisons. Climate Dynamics, 49(5-6), 1665-1679.

Bakun, A., (1973). Coastal upwelling indices, west coast of North America, 1946-71. U.S.Dep. Commer., NOAA Tech. Rep., NMFS SSRF-671, 103 p.

Bricaud, A., A. Morel, and J.-M. Andre´ (1987). Spatial/temporal variability of algal biomass in the mauritanian upwelling zone, as estimated from CZCS data, Adv. Space Res.,7(2), 53–62.

Brodeau, L., Barnier, B., Treguier, A. M., Penduff, T., &Gulev, S. (2010). An ERA40-based atmospheric forcing for global ocean circulation models. Ocean Modelling, 31(3-4), 88-104.

Carton, J. A., Chepurin, G. A., & Chen, L. (2018). SODA3: A new ocean climate reanalysis. Journal of Climate, 31(17), 6967-6983

Castelao, R. M., and Y. Wang (2014). Wind-driven variability in sea surface temperature front distribution in the California Current System, J. Geophys. Res. Oceans, 119, 1861– 1875, doi:10.1002/2013JC009531.

Chang, P., L. Ji, and H. Li (1997). A decadal climate variation in the tropical Atlantic Ocean from thermodynamic air-sea interactions, Nature, 385, 516– 518.

Compo, G.P., et al. (2011). The Twentieth Century Reanalysis Project. Quarterly Journal of the Royal Meteorological Society, 137, 1-28. http://dx.doi.org/10.1002/qj.776

Cropper, T. E., Hanna, E., & Bigg, G. R. (2014). Spatial and temporal seasonal trends in coastal upwelling off Northwest Africa, 1981–2012. Deep Sea Research Part I: Oceanographic Research Papers, 86, 94-111.

Dee, D. P., Uppala, S. M., Simmons, A. J., Berrisford, P., Poli, P., Kobayashi, S., ... & Vitart, F. (2011). The ERA Interim reanalysis: Configuration and performance of the data assimilation system. Quarterly Journal of the royal meteorological society, 137(656), 553-597

Diakhaté, M., De Coëtlogon, G., Lazar, A., Wade, M., & Gaye, A. T. (2016). Intraseasonal variability of tropical Atlantic sea-surface temperature: air–sea interaction over upwelling fronts. Quarterly Journal of the Royal Meteorological Society, 142(694), 372-386. Doi: https://doi.org/10.1002/qj.2657

Dieppois, B., Durand, A., Fournier, M., Diedhiou, A., Fontaine, B., Massei, N., ... &Sebag, D. (2015). Low-frequency variability and zonal contrast in Sahel rainfall and Atlantic sea surface temperature teleconnections during the last century. Theoretical and Applied Climatology, 121(1-2), 139-155.

Dong, B., Sutton, R. T., & Scaife, A. A. (2006). Multidecadal modulation of El Nino–Southern Oscillation (ENSO) variance by Atlantic Ocean sea surface temperatures. Geophysical Research Letters, 33(8).

Duchon C. E. (1979). Lanczos Filtering in One and Two Dimensions. Journal of Applied Meteorology, Vol 18, pp 1016-1022.

Enfield, D.B., and Mayer, D.A., (1997). Tropical Atlantic SST variability and its relation to El Niño-Southern Oscillation.Journal of Geophysical Research,102, 929–945.

Faye, S., Lazar, A., Sow, B. A., & Gaye, A. T. (2015). A model study of the seasonality of sea surface temperature and circulation in the Atlantic North-eastern Tropical Upwelling System. Frontiers in Physics, 3, 76.

Fedorov, A. V., & Philander, S. G. (2000). Is El Niño changing? Science, 288(5473), 1997-2002.

Florenchie, P., J.R.E. Lutjeharms, C.J.C. Reason, S. Masson, and M. Rouault. (2003). The source of Benguela Niños in the South Atlantic Ocean, Geophys. Res. Lett. 30, (10), 1505, doi:10.1029/2003GL017172.

Foltz, G. R., Brandt, P., Richter, I., Rodríguez-Fonseca, B., Hernandez, F., Dengler, M., ... & Reul, N. (2019). The tropical Atlantic observing system. Frontiers in Marine Science, 6, 206.

García-Serrano J., C. Cassou, H. Douville, A. Giannini, F. J. Doblas-Reyes (2017). Revisiting the ENSO teleconnection to the tropical North Atlantic. J. Clim, 0894-8755. DOI: 10.1175/JCLI-D-16-0641.1.

Giese, B. S., & Ray, S. (2011). El Niño variability in simple ocean data assimilation (SODA), 1871–2008. Journal of Geophysical Research: Oceans, 116(C2).

Giese, B. S., Seidel, H. F., Compo, G. P., &Sardeshmukh, P. D. (2016). An ensemble of ocean reanalyses for 1815–2013 with sparse observational input. Journal of Geophysical Research: Oceans, 121(9), 6891-6910.

Graham NE (1994). Decadal-scale climate variability in the tropical and North Pacific during the 1970s and 1980s: observations and model results. Climate Dynamics 10:135-162. https://doi.org/10.1007/BF00210626

Guilderson TP, Schrag DP (1998). Abrupt Shift in Subsurface Temperatures in the Tropical Pacific Associated with Changes in El Niño. Science 281:240-243. https://doi.org/10.1126/science.281.5374.240

Herbland, A., and B. Voituriez (1974). La production primaire dans l'upwelling mauritanien en mars 1973,Cah. O.R.S.T.O.M., sér. Océanogr.,12(3), 187–201.

Huntsman, S. A., and R. T. Barber (1977). Primary production off north-west Africa: The relationship to wind and nutrient conditions,Deep SeaRes.,24, 25–33.

Illig, S., and Bachèlery, M. L. (2019). Propagation of subseasonal equatorially-forced coastal trapped waves down to the benguela upwelling system. Sci. Rep. 9:5306. doi: 10.1038/s41598-019-41847-1.

Jacox, M. G., Edwards, C. A., Hazen, E. L., and Bograd, S. J. (2018). Coastal upwelling revisited: ekman, bakun, and improved upwelling indices for the U.S. West Coast. J. Geophys. Res. 123, 7332–7350. doi: 10.1029/2018JC014187

Kessler, W. S., M. J. McPhaden, and K. M. Weickmann (1995). Forcing of intraseasonal Kelvin waves in the equatorial Pacific, J. Geophys. Res., 100, 10,613– 10,631.

Knight, J. R., Folland, C. K., & Scaife, A. A. (2006). Climate impacts of the Atlantic multidecadal oscillation. *Geophysical Research Letters*, *33*(17).

Lee, S. K., Enfield, D. B., & Wang, C. (2008). Why do some El Niños have no impact on tropical North Atlantic SST? Geophysical Research Letters, 35(16).

Levine, A. F., McPhaden, M. J., & Frierson, D. M. (2017). The impact of the AMO on multidecadal ENSO variability. Geophysical Research Letters, 44(8), 3877-3886.

López-Parages, J., & Rodríguez-Fonseca, B. (2012). Multidecadal modulation of El Niño influence on the Euro-Mediterranean rainfall. Geophysical Research Letters, 39(2).

López-Parages, J., Rodríguez-Fonseca, B., &Terray, L. (2015). A mechanism for the multidecadal modulation of ENSO teleconnection with Europe. Climate Dynamics, 45(3-4), 867-880.

López-Parages, J., Rodríguez-Fonseca, B., Dommenget, D., &Frauen, C. (2016). ENSO influence on the North Atlantic European climate: a non-linear and non-stationary approach. Climate Dynamics, 47(7-8), 2071-2084.

Losada, T., Rodríguez-Fonseca, B., Mohino, E., Bader, J., Janicot, S., & Mechoso, C. R. (2012). Tropical SST and Sahel rainfall: A non-stationary relationship. Geophysical Research Letters, 39(12).

Lübbecke, J. F., C. W. Böning, N. S. Keenlyside, and S.P. Xie (2010), On the connection between Benguela and equatorial Atlantic Niños and the role of the South Atlantic Anticyclone, J. Geophys. Res., 115, C09015, doi:10.1029/2009JC005964.

Mariotti, A., Zeng, N., & Lau, K. M. (2002). Euro-Mediterranean rainfall and ENSO—a seasonally varying relationship. Geophysical research letters, 29(12), 59-1.

Martín-Rey, M., Polo, I., Rodríguez-Fonseca, B., Losada, T., & Lazar, A. (2018). Is there evidence of changes in tropical Atlantic variability modes under AMO phases in the observational record? Journal of Climate, 31(2), 515-536.

Martín-Rey, M., Polo, I., Rodríguez-Fonseca, B., Lazar, A., & Losada, T. (2019). Ocean dynamics shapes the structure and timing of Atlantic Equatorial Modes. Journal of Geophysical Research: Oceans.

McPhaden, M. J., (1999). Genesis and evolution of the 1997–1998 El Niño,Science, 283, 950–954.

Monterey, G. I., and S. Levitus, (1997). Seasonal Variability of Mixed Layer Depth for the World Ocean. NOAA Atlas NESDIS 14, 5 pp. and 87 figs

Ndoye, S., X. Capet, P. Estrade, B. Sow, D. Dagorne, A. Lazar, A. Gaye, and P. Brehmer (2014). SST patterns and dynamics of the southern Senegal-Gambia upwelling center, J. Geophys. Res. Oceans, 119, 8315–8335, doi:10.1002/2014JC010242.

Nitta T, Yamada S (1989). Recent Warming of Tropical Sea Surface Temperature and Its Relationship to the Northern Hemisphere Circulation. Journal of the Meteorological Society of Japan Ser II 67:375-383. https://doi.org/10.2151/

Nykjaer, L., and L. Van Camp (1994). Seasonal and interannual variability of coastal upwelling along northwest Africa and Portugal from 1981 to 1991, J. Geophys. Res.,99(C7), 14,197–14,207.

Oettli, P., Y. Morioka, and T. Yamagata, (2016). A regional climate mode discovered in the North Atlantic: Dakar Niño/Niña. Sci.Rep.,6, 18782, doi:10.1038/srep18782.

Okumura Y, Xie SP (2006). Some overlooked features of tropical Atlantic climate leading to a new Niño-like phenomenon. J Clim 19(22):5859–5874.

Polo, I., B. R. de Fonseca, and J. Sheinbaum (2005). Northwest Africa upwelling and the Atlantic climate variability, Geophys. Res. Lett.,32, L23702, doi:10.1029/2005GL023883.

Polo, I., A. Lazar, B. Rodriguez-Fonseca, and S. Arnault (2008). Oceanic Kelvin waves and tropical Atlantic intraseasonal variability: 1. Kelvin wave characterization, J. Geophys. Res., 113, C07009, doi:10.1029/2007JC004495.

Rayner, N. A. A., Parker, D. E., Horton, E. B., Folland, C. K., Alexander, L. V., Rowell, D. P., ... & Kaplan, A. (2003). Global analyses of sea surface temperature, sea ice, and night marine air temperature since the late nineteenth century. *Journal of Geophysical Research: Atmospheres*, *108*(D14).

Rodríguez-Fonseca, B., Janicot, S., Mohino, E., Losada, T., Bader, J., Caminade, C., ... & Joly, M. (2011). Interannual and decadal SST-forced responses of the West African monsoon. AtmosphericScienceLetters, 12(1), 67-74.

Rodríguez-Fonseca, B., Mohino, E., Mechoso, C. R., Caminade, C., Biasutti, M., Gaetani, M., ... & Polo, I. (2015). Variability and predictability of West African droughts: a review on the role of sea surface temperature anomalies. Journal of Climate, 28(10), 4034-4060.

Roy, C. and C. Reason. (2001). ENSO related modulation of coastal upwelling in the eastern Atlantic. Prog. Oceanogr., 49, 245–255.

Santos, M. P., A. S. Kazmin, and A. Peliz (2005). Decadal changes in theCanary upwelling system as revealed by satellite observations: Their impact on productivity, J. Mar. Res.,63, 359–379.

Suárez-Moreno, R., Rodríguez-Fonseca, B., Barroso, J. A., & Fink, A. H. (2018). Interdecadal changes in the leading ocean forcing of Sahelian rainfall interannual variability: atmospheric dynamics and role of multidecadal SST background. Journal of Climate, 31(17), 6687-6710.

Sutton, R. T., S. P. Jewson, and D. P. Rowell, (2000). The elements of cli-mate variability in the tropical Atlantic region. J. Climate,13,3261–3284.

Sylla, A., Mignot, J., Capet, X., & Gaye, A. T. (2019). Weakening of the Senegalo–Mauritanian upwelling system under climate change. Climate Dynamics, 53(7), 4447-4473

Taschetto, A. S., Rodrigues, R. R., Meehl, G. A., McGregor, S., & England, M. H. (2016). How sensitive are the Pacific–tropical North Atlantic teleconnections to the position and intensity of El Niño-related warming?. Climate Dynamics, 46(5), 1841-1860.

Terray P (1994). An Evaluation of Climatological Data in the Indian Ocean Area. Journal of the Meteorological Society of Japan 72:359-386. https://doi.org/10.2151/jmsj1965.72.3_359

Trenberth KE, Hurrell JW (1994). Decadal atmosphere-ocean variations in the Pacific. Clim Dyn 9:303-319. https://doi.org/10.1007/BF00204745

Uppala, S. M., Kållberg, P. W., Simmons, A. J., Andrae, U., Bechtold, V. D. C., Fiorino, M., ... &Woollen, J. (2005). The ERA-40 re-analysis. Quarterly Journal of the Royal Meteorological Society: A journal of the atmospheric sciences, applied meteorology and physical oceanography, 131(612), 2961-3012.

Van Camp, L., L. Nykjaer, E. Mittelstaedt, and P. Schlittenhardt (1991).Upwelling and boundary circulation off northwest Africa as depicted by infrared and visible satellite observations,Prog. Oceanogr.,26, 357–402.

Wang C. (2002a). Atlantic climate variability and its associated atmospheric circulation cells. Journal of Climate 15:1516 – 1536.

Wang, C. Z., (2006). An overlooked feature of tropical climate: Inter-Pacific–Atlantic variability. Geophys. Res. Lett., 33, L12702, https://doi.org/10.1029/2006GL026324.

Wilks, D. S. (2011). Statistical methods in the atmospheric sciences (Vol. 100). Academic press.

Wooster, W., A. Bakun, and D. McLain (1976). The seasonal upwelling cycle along the eastern boundary of the north Atlantic, J. Mar. Res.,34,131–141.

Xie, S.-P., and S. G. H. Philander (1994). A coupled ocean-atmosphere model of relevance 12to the ITCZ in the eastern Pacific. Tellus 46A, 340–350.

Zhang, C., (2001). Intraseasonal perturbations in sea surface temperatures of the equatorial eastern Pacific and their association with the Madden-Julian Oscillation, J. Clim., 14, 1309–1322, 2001.

Zhang, W., Mei, X., Geng, X., Turner, A. G., & Jin, F. F. (2019). A Nonstationary ENSO–NAO Relationship Due to AMO Modulation. Journal of Climate, 32(1), 33-43.

Zuo, H., Balmaseda, M. A., Tietsche, S., Mogensen, K., & Mayer, M. (2019). The ECMWF operational ensemble reanalysis–analysis system for ocean and sea ice: a description of the system and assessment. Ocean science, 15(3), 779-808.

Additional Material

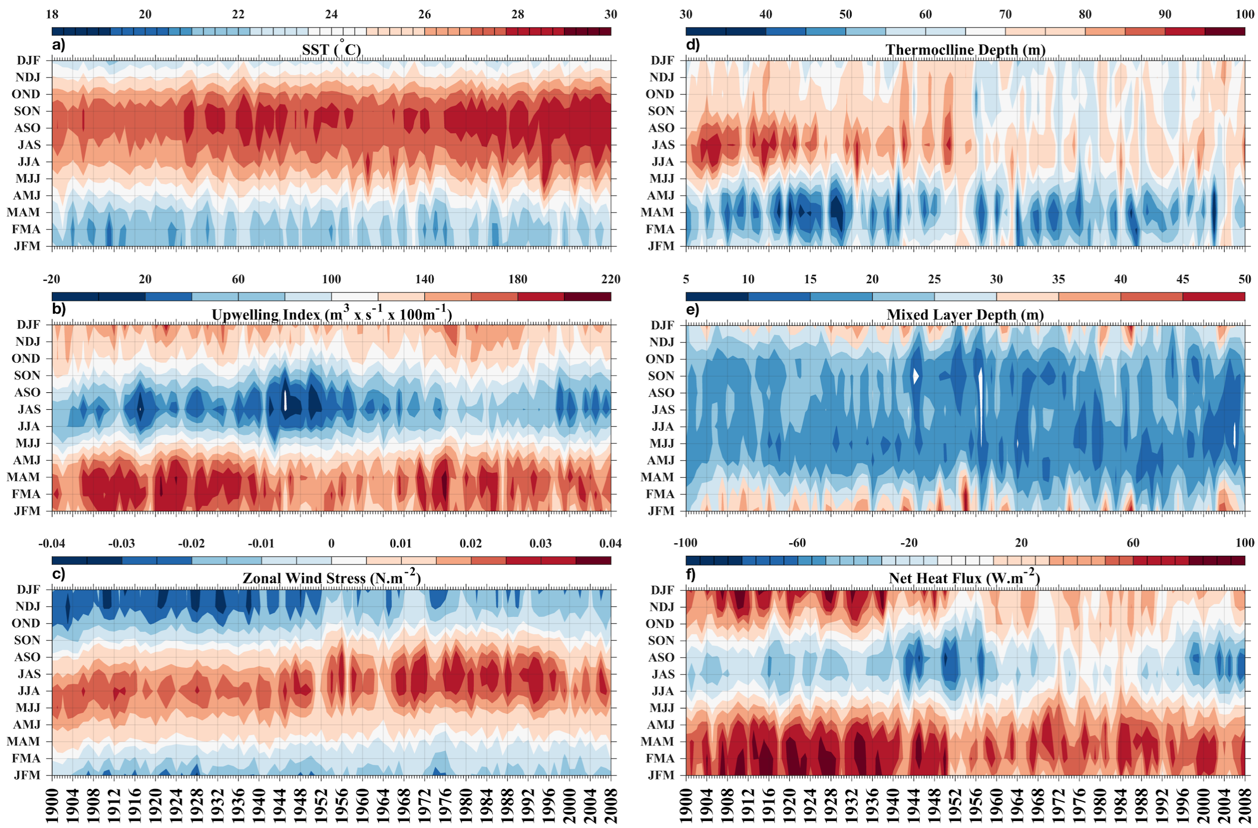

Figure 1: Variations in the seasonal cycle of: a) SST, b) Upwelling index, c) Zonal wind stress, d) Thermocline depth (THD), e) mixed layer depth (MLD), and f) net heat flux indexes averaged in the upwelling area, SCU (18°W-17°W and 12°N-16°N). Note that, positive heat fluxes indicate that the ocean is gaining heat from the atmosphere and vice versa. The period of the study is from 1900 to 2008.